EGF inhibits constitutive internalization and palmitoylation-dependent degradation of membrane spanning pro-cancer CDCP1 promoting its availability on the cell surface

Mark N. Adams[1], Brittney S. Harrington[1], Yaowu He[1], Claire M. Davies[1,2], Sarah J. Wallace[2], Naven P. Chetty[2], Alexander J. Crandon[2], Niara B. Oliveira[2], Catherine M. Shannon[2], Jermaine I. Coward[1,2], John W. Lumley[3], Lewis C. Perrin[2], Jane E. Armes[1,2] and John D. Hooper[1]

[1]Mater Research Institute-University of Queensland, Translational Research Institute, Woolloongabba, Australia; [2]Mater Health Services, South Brisbane, Australia and [3]Wesley Hospital, Auchenflower, Australia. Correspondence: John D Hooper, [1]Mater Research Institute-University of Queensland, Translational Research Institute, 37 Kent Street, Woolloongabba Qld 4102, Australia.
E-mail: john.hooper@mater.uq.edu.au.

ABSTRACT

Many cancers are dependent on inappropriate activation of epidermal growth factor receptor (EGFR) and drugs targeting this receptor can improve patient survival, although benefits are generally short-lived. We reveal a novel mechanism linking EGFR and the membrane spanning, cancer promoting protein CDCP1. Under basal conditions cell surface CDCP1 constitutively internalizes and undergoes palmitoylation-dependent degradation by a mechanism in which it is palmitoylated on at least one of its four cytoplasmic cysteines. This mechanism is functional *in vivo* as CDCP1 is elevated and palmitoylated in high grade serous ovarian tumors. Interestingly, activation of the EGFR system with EGF inhibits proteasome-mediated, palmitoylation-dependent degradation of CDCP1, promoting recycling of CDCP1 to the cell surface where it is available to mediate its pro-cancer effects. We also show that mechanisms inducing relocalization of CDCP1 to the cell surface, including disruption of its palmitoylation and EGF treatment, promote cell migration. Our data provide the first evidence that the EGFR system can function to increase the lifespan of a protein and also promote its recycling to the cell surface. This information may be useful for understanding mechanisms of resistance to EGFR therapies and assist in the design of treatments for EGFR-dependent cancers.

Keywords: EGF, EGFR, CDCP1, cancer

INTRODUCTION

Epidermal growth factor receptor (EGFR) is a tyrosine kinase that modulates cell survival, proliferation, migration and neovascularization (1). Its inappropriate activation is a common event in cancer and inhibitors and antibodies targeting it are used to treat non-small-cell lung cancer (NSCLC) and cancer of the head and neck, colon and rectum, and pancreas (1-3). However, most tumors have intrinsic mechanisms to circumvent blockade of EGFR signaling or acquire resistance over relatively short periods. Additional mechanistic insights into EGFR signalling are expected to lead to new paradigms for treatment of malignancies dependent on this pathway (2, 3).

CUB domain containing protein 1 (CDCP1) is a 135 kDa transmembrane protein that can be proteolytically processed to 70 kDa (4-6). It was isolated using an approach biased to identify proteins involved in metastasis (7) and consistent with a role in aggressive cancer, elevated CDCP1 correlates with poor outcome in kidney (8-10), pancreatic (11), lung (12) and colon and rectum (13) cancer. Also, CDCP1 mRNA is significantly elevated in ovarian cancer (9). Animal models suggest functional roles for CDCP1 in cancer. CDCP1 silencing reduces vascular dissemination in mice of lung cancer (14) and melanoma (15) cell lines, and disrupts peritoneal metastasis of gastric cancer cells (16) while its over-expression increases metastasis of cervical cancer cells (17) and poorly metastatic melanoma cells (15). Antibody targeting of CDCP1 is effective at reducing vascular dissemination *in vivo* of prostate cancer and CDCP1 over-expressing cell lines (17-20) and also efficiently inhibits subcutaneous growth in mice of established human cell line xenograft tumors (21). Also, cytotoxin-conjugated anti-CDCP1 antibodies markedly reduce lymphatic dissemination of prostate cancer cells (22). Mechanistically CDCP1 promotes cell survival *in vivo* via an Akt-mediated pathway which is blocked by CDCP1 targeting monoclonal antibodies resulting in cell death (17-19). Other studies propose that monoclonal antibodies against CDCP1 may be beneficial for treatment of a range of malignancies (9, 10).

Recent reports link EGFR and CDCP1. EGFR activation increases CDCP1 expression in serous ovarian cancer cell lines, and induces its redistribution during migration from cell-cell

junctions to filopodia and intracellular locations that likely replenish the cell surface (23). Inhibition of CDCP1 function through silencing and function blocking antibodies effectively reduces EGF-induced migration also supporting that targeting of CDCP1 may be useful in controlling ovarian cancer response to EGF/EGFR signaling (23). In addition, data from 732 cancer cell lines reveals high concordance in CDCP1 and EGFR mRNA expression suggesting that cancers dependent on EGFR will have elevated CDCP1 (9). Here we examine EGFR mechanisms regulating CDCP1 with our data demonstrating the first example of the EGFR system functioning to increase the lifespan and cell surface availability of a protein.

RESULTS

EGF protects CDCP1 from degradation

We have shown that CDCP1 mediates EGFR-induced cell migration (23) via a mechanism involving CDCP1 relocalization from cell-cell junctions to filopodia and intracellular punctate structures (23). To further explore this mechanism, we examined the lifespan of CDCP1 in response to the EGFR ligand EGF (24) by tracking biotinylated cell surface proteins over time. In both unstimulated OVCA420 and Caov3 ovarian cancer cells, after 12 h the level of biotinylated CDCP1 was less than 5% of levels apparent immediately after cell surface biotinylation (Figure 1A), indicating that the cell surface localized protein is constitutively degraded. In contrast, EGF protected CDCP1 from degradation with >80% of starting levels apparent after 12 h (Figure 1A). To explore whether other signaling proteins alter CDCP1 lifespan, the assay was repeated using OVCA420 cells treated with interleukin(IL)-6 and tumour necrosis factor alpha (TNFα) which are important in the inflammatory cytokine network in the ovarian cancer microenvironment (25). In contrast with EGF, IL-6 and TNFα failed to protect cell surface CDCP1 from protein turn-over (Figure 1B).

CDCP1 is palmitoylated *in vitro* and *in vivo*

Examination of the CDCP1 amino acid sequence for motifs potentially regulating EGF-induced effects, identified a putative palmitoylation motif at di-cysteine 689 (C689)/C690, which is proximal to its transmembrane domain at residues 666-686, as well as cysteines at C772 and C780 (Figure 2A). As addition of palmitate affects protein stability (26), these sites were of interest as regulators of EGF-induced increased CDCP1 lifespan. To first address whether CDCP1 is palmitoylated, we used an acyl-biotinyl exchange assay in which

palmitoylated cysteines on proteins present within membrane fractions are labelled with biotin then captured using streptavidin beads before detection by Western blot analysis (27, 28). This demonstrated that both full length 135 kDa and proteolytically processed 70 kDa CDCP1 are palmitoylated in both Caov3 and OVCA420 cells as well as in cells from prostate, ovarian, gastric, kidney and lung cancer (Figure 2B). In each cell line CDCP1 was palmitoylated in direct proportion to its level of expression. The known palmitoylated protein caveolin-1 (CAV1) (29) was used as a control in cells known to express this protein.

The potential significance of palmitoylated CDCP1 was explored by examining its expression *in vivo*. Subcutaneous (Figure 2C, left) and intraperitoneal (Figure 2C, right) ovarian cancer SKOV3 cell tumors expressed 135 kDa CDCP1 exclusively and this form of the protein was palmitoylated as was seen for *in vitro* cultured SKOV3 cells (Figure 2C, lower). We also examined CDCP1 in prospectively collected benign and malignant ovarian samples including tumors from 9 women with high grade serous ovarian cancer and ovarian tissue from 7 women with benign disorders (Table S1). CDCP1 was either undetectable or barely detectable in benign ovarian tissue, whereas each malignant sample expressed both full-length 135 kDa and proteolytically processed 70 kDa CDCP1 (Figure 2D). Except for samples from 2 patients (lane 16 and 18) palmitoylation of each malignant sample was directly proportional to the level of CDCP1 expression. Interestingly, both of the exceptions were metastases. One was a pelvic metastasis (lane 16) and the other an omental metastasis collected after chemotherapy (lane 18). In contrast with the metastasis, for both patients the level of palmitoylated CDCP1 in the matching primary tumor was directly proportional to CDCP1 expression (lane 15 and 17). To examine whether palmitoyaltion of CDCP1 was generally not proportional to its level of expression in metastases, we examined total and palmitoylated CDCP1 in another 4 prospectively collected matched primary tumors and omental metastases. As shown in Figure 2E, the level of CDCP1 was elevated in the metastasis of one of these patients and reduced in the other three. In the patient with elevated CDCP1 in the metastasis there was proportionally much lower palmitoylated CDCP1 than in the matching primary tumor. For the other 3 patients, even though there were markedly lower levels of CDCP1 in the metastases, these samples were almost devoid of palmitoylated CDCP1; in contrast the matching primary tumours showed relatively high levels of palmitoylated CDCP1 (Figure 2E, lower). Taking into account the altered expression of CDCP1 in the metastases relative to the primary tumors, it is apparent that for each of the 6 analyzed patients the level of palmitoylated CDCP1 was markedly lower in the metastasis.

These data indicate that CDCP1 is upregulated in primary high grade serous ovarian tumours and its palmitoylation and, potentially, expression are decreased at metastatic sites.

To explore the role of palmitoylation in increased EGF-induced CDCP1 lifespan, we first identified those cysteines that can be palmitoylated. For this purpose we systematically mutated to alanine each of the four CDCP1 cysteines, each of the 6 possible double and 4 possible triple mutants as well as the quadruple mutant referred to as CDCP1-4C. Acyl-biotinyl exchange assays demonstrated that it is only when all 4 sites are mutated that CDCP1 palmitoylation is completely abolished (Figure 2F).

EGF inhibits palmitoylation-dependent proteasomal degradation of CDCP1 promoting its recycling to the cell surface

To assess the impact of palmitoylation and EGF treatment on the lifespan of CDCP1, transiently transfected HeLa cells showing similar cell surface expression of wildtype and palmitoylation-deficient CDCP1 (Figure 3A, left), were labelled with biotin and their degradation followed over time. Under basal conditions over 24 h the level of CDCP1 gradually reduced to ~10% of controls (Figure 3A). In contrast, ~60% of palmitoylation-deficient CDCP1-4C remained (Figure 3A) demonstrating the importance of palmitoylation in CDCP1 degradation. Interestingly, EGF had a marked effect on the lifespan of wildtype but not palmitoylation-deficient CDCP1. Over 12 h EGF treatment markedly reduced degradation of CDCP1 with levels approximately the same as CDCP1-4C under basal and EGF treatment conditions (Figure 3B). Collectively these data demonstrate that CDCP1 lifespan is regulated by EGF and palmitoylation; EGF increases CDCP1 lifespan and palmitoylation is required for its efficient degradation.

To further examine the effect of palmitoylation on CDCP1, we followed internalization of wildtype and palmitoylation deficient CDCP1 under basal conditions using a biotinylation internalization assay (30). In this assay internalization of cell surface biotinylated proteins is followed for 0.5, 1, 2 and 8 h. Chemical removal of residual cell surface biotin tagged proteins before cell lysis using 2-mercaptoethanesulfonic acid sodium salt (MeSNA) ensures Western blot analysis detects only protein trafficked to the cytoplasm (Figure 3C, upper). A maximum period of 8 h was selected to avoid the near complete degradation of CDCP1 apparent at later time points in Figure 3A-B. Similar levels of trafficked CDCP1 and CDCP1-

4C were apparent after 2 h suggesting that palmitoylation is not required for internalization (Figure 3C, middle). However, after 8 h CDCP1 levels were reduced to ~20% of levels apparent immediately after cell surface biotinylation, whereas CDCP1-4C levels were ~80% of starting levels. Co-incubation of cells with the proteasome inhibitor MG132 increased CDCP1 levels to the level seen for CDCP1-4C, suggesting that the reduced levels of CDCP1 were due to its proteasomal degradation rather than recycling to the plasma membrane (Figure 3C, lower). These data indicate that while palmitoylation is not essential for CDCP1 internalization, it is required for its degradation which is mediated by the proteasome.

To examine the effect of EGF on the observed palmitoylation-independent internalization and palmitoylation-dependent degradation of CDCP1, we compared internalization and recycling to the cell surface of wildtype and palmitoylation-deficient CDCP1 using a modified version of the biotinylation internalization assay. Plasma membrane proteins were biotinylated at 4°C, then cells were either untreated or treated with EGF for 1 h at 37°C before MeSNA treatment to remove residual cell surface biotinylated proteins. Cells were then either processed as described above for Western blot analysis of streptavidin purified biotinylated proteins to identify internalized CDCP1, or incubated for a further 1 h at 37°C in the presence or absence of EGF before a second round of MeSNA treatment to remove biotinylated proteins that had recycled to the cell surface (Figure 3D, upper). Anti-CDCP1 Western blot analysis of streptavidin purified biotinylated proteins from the cells subjected to the additional MeSNA treatment revealed levels of CDCP1 that had not recycled to the plasma membrane. It was apparent from these approaches that at 1 h CDCP1 internalization was unaffected by EGF stimulation and the rate of internalization was unaffected by palmitoylation (Figure 3D, middle). In contrast, the level of CDCP1 that remained internalized after returning the cells to 37°C for 1 h was markedly affected by both palmitoylation and EGF. While ~55% of CDCP1-4C recycled to the cell surface in unstimulated cells, most of the wildtype CDCP1 remained internalized. EGF increased by ~3 fold (from ~15% to ~45%) the amount of CDCP1 that recycled to the cell surface, whereas there was a reduction from ~55% to ~40% of CDCP1-4C that recycled (Figure 3D, lower). These data suggest that while palmitoylation is not required for CDCP1 internalization, which occurs constitutively, it is needed for its for degradation, and without palmitoylation CDCP1 constitutively recycles back to the cell surface. In addition, the data provide a mechanistic rationale for the observations in Figure 1a, 3b and 3cC, that EGF is able to reduce CDCP1 degradation. It appears that this occurs because EGF redirects trafficking of

CDCP1 away from palmitoylation-dependent proteasomal degradation towards recycling to the plasma membrane.

EGF reduces CDCP1 palmitoylation and promotes its redistribution into non-lipid raft membrane fractions

To directly examine the effect of EGF on palmitoylation of CDCP1, we monitored the level of palmitoylated and total CDCP1 in response to EGF treatment over 24 h. As in Figure 2B, in this assay palmitoylated proteins present within membrane fractions are labelled using an acyl-biotinyl exchange assay then captured for Western blot analysis using streptavidin beads. In this way we follow the accumulation of palmitoylated CDCP1 in response to EGF. Up to 12 h the levels of palmitoylated CDCP1 increased at the same rate as total CDCP1 in both OVCA420 and Caov3 cells meaning that the ratio of palmitoylated to total CDCP1 remained constant (Figure 4A, upper). However, between 12 and 24 h there was a ~5 fold reduction in this ratio (Figure 4A, lower). To uncouple the effect of EGF on CDCP1 expression from its impact on CDCP1 palmitoylation, we repeated EGF treatment on HeLa cells transiently expressing CDCP1. As shown in Figure 4B, levels of CDCP1 palmitoylation were reduced as early as 6 h after commencement of EGF stimulation with marked reduction apparent at 24 h. These data suggest that in cells endogenously expressing CDCP1, there is a balance between, on the one hand, EGF-induced synthesis (23) and non-palmitoylation-mediated cellular processing of new CDCP1, and, on the other hand, its palmitoylation and degradation. Up to 12 h after EGF treatment commences, these processes are evenly balanced resulting in a constant ratio of palmitoylated to total CDCP. However, between 12 and 24 h the kinetics of EGF-induced new protein synthesis coupled with the recycling of CDCP1 seen in Figure 3C-D, predominates over the kinetics of palmitoylation-dependent degradation, resulting in much lower levels of palmitoylated CDCP1 relative to total CDCP1.

Palmitoylation also regulates protein location within plasma membrane microdomains, promoting association with cholesterol- and sphingolipid-rich regions, called lipid rafts (26). Recently CDCP1 has been localized to lipid rafts of breast cancer MDA-MB-231 cells (31). We examined the distribution of CDCP1 and the lipid raft marker Flottilin-1 in low density lipid raft-enriched and high density lipid raft-poor membrane fractions isolated from untreated and EGF treated Caov3 cells. At 24 h CDCP1 in untreated cells predominated in lipid raft-enriched fractions while EGF caused a shift to predominant localisation in lipid raft-

poor fractions (Figure 4C). Quantitative densitometric analysis showed a shift from only ~20% of CDCP1 being present in lipid raft-poor fraction 4 from unstimulated Caov3, to about 65% in EGF-stimulated cells. As the kinase Src, which is the key mediator of tyrosine phosphorylation of CDCP1 (7, 14, 32), is found in lipid rafts and differentially signals within and outside these structures (33), we were interested to examine the impact of EGF on phosphotyrosine-CDCP1 (pY-CDCP1). CaOV3 and OVCA420 cells were incubated with EGF for 6, 12 and 24 h before immunoprecipitation of CDCP1 and detection of pY-CDCP1 using an anti-phosphotyrosine antibody. As shown in Figure 4D, pY-CDCP1 levels dropped gradually in both cell lines in response to EGF. OVCA420 cells showed a 22% reduction after 6 h with levels plateauing at about a 70% reduction after 12 h through to 24 h. In contrast, after 6 h there was actually a 26% increase in pY-CDCP1 levels in CaOV3 cells with levels dropping to 55% of untreated levels after 24 h (Figure 4D). Collectively, the data in Figure 4 demonstrate that EGF reduces both palmitoylation and tyrosine phosphorylation of CDCP1 over 24 h treatment periods and this is accompanied by relocation of CDCP1 out of lipid rafts. The data suggest that EGF switches CDCP1 from its default pathway involving internalization and palmitoylation-dependent degradation, towards a pathway in which it moves out of lipid rafts and recycles to the cell surface avoiding degradation. Reduced levels of pY-CDCP1 are consistent with EGF-induced movement of CDCP1 away from the membrane micro-domains known to harbor the key mediator of CDCP1 phosphorylation, Src.

Palmitoylation retards basal and EGF-induced CDCP1-mediated cell migration

Our data indicate that EGF increases lifespan and cell surface availability of CDCP1, likely via a mechanism where it is switched from its default internalization and palmitoylation-dependent degradation. To examine the potential functional importance of these observations, we assessed the impact of loss of CDCP1 palmitoylation on the EGF-induced CDCP1-mediated cell migration previously described by us (23). After 48 h migration of unstimulated cells was ~4 and ~5 fold higher, respectively, in HeLa-CDCP1 and HeLa-CDCP1-4C cells compared with HeLa-vector cells (Figure 5). In addition, migration of EGF treated cells was ~2 and ~4 fold higher in HeLa-CDCP1 and HeLa-CDCP1-4C cells, respectively, compared with HeLa-vector cells (Figure 5). These data are consistent with both EGF and loss of palmitoylation increasing the availability of CDCP1 at the cell surface where it can mediate basal and EGF-induced cell migration. The data would suggest that palmitoylation-deficient

CDCP1 is more readily available to promote cell migration than palmitoylation capable CDCP1.

DISCUSSION

We report a new EGF-regulated molecular mechanism that may be useful for defining strategies to target EGFR-dependent tumors. As summarized in Figure 6, constitutive internalization of cell surface localized, membrane spanning CDCP1, and its proteasome-mediated degradation, are inhibited by the EGFR ligand EGF. EGF increases the lifespan of CDCP1 promoting its availability on the cell surface where our data indicate it is available to mediate pro-cancer phenotypes such as cell migration. Based on published analysis of patient cohorts and animal models, antibody targeting of CDCP1 has been proposed for cancer treatment (9, 10, 18, 20). This is supported by molecular analysis demonstrating that CDCP1 is pro-cancerous *in vivo* by promoting cell survival via pathways involving Src, PKCδ, FAK, PI3K and Akt (14, 18, 19), and that anti-CDCP1 antibodies efficiently block survival, inducing apoptosis (18-20, 22). It is also supported by a recent mechanistic study showing that an anti-CDCP1 monoclonal antibody that induces lipid raft translocation, internalization and degradation of CDCP1, blocked subcutaneous growth in mice of established human cell line xenograft tumors (21).

The greatest potential for antibody-based drugs targeting CDCP1 will be in tumors where it is available on the cell surface, including potentially EGFR-dependent malignancies. At least in cell lines the EGFR system up-regulates CDCP1 expression (23) and also increases its lifespan and location on the plasma membrane. Based on recent reports, NSCLC patients may be the most likely to benefit from anti-CDCP1 antibodies, potentially in combination with EGFR targeted drugs, as ~60% of these patients positive for EGFR mutation respond to EGFR inhibition (34), and elevated expression of CDCP1 correlates with poorer disease-free and overall survival of NSCLC patients (12).

Our data showing that CDCP1 is up-regulated via the EGFR system is supported by a recent report demonstrating that levels of the encoding transcripts are highly correlated across 732 cancer cell lines (9). Interestingly, high correlation across this large cell line dataset was also seen between CDCP1 mRNA, and transcripts encoding the transcription factor hypoxia-inducible factor (HIF)-2α and the receptor tyrosine kinase Met, indicating that cancers with

high HIF-2α or Met expression will likely have high CDCP1 levels (9). Consistently, recent papers have linked HIF-2α and CDCP1 (9, 10). Razorenova et al showed that CDCP1 is markedly upregulated by hypoxia in clear cell renal cell carcinoma (ccRCC) cell lines via HIF-1α and HIF-2α. This group also highlighted the importance of cell surface CDCP1 with survival analysis of 50 ccRCC patients showing that 50% of patients positive for plasma membrane CDCP1 were dead by 7.5 years, whereas >75% of patients with negative or cytoplasmic CDCP1 were alive at the end of follow-up at ~12 years (10). Emerling et al also showed that HIF-2α regulates CDCP1 expression in breast and melanoma cell lines with HIF-2α binding to the *CDCP1* promoter in complex with the aryl hydrocarbon nuclear translocator (9). Accordingly, CDCP1 is regulated by the well-known cancer promoting systems EGFR and HIF, and potentially Met.

Consistent with a recent report showing that CDCP1 mRNA is significantly elevated in ovarian cancer (9), we observed that CDCP1 protein is markedly upregulated in primary high grade serous ovarian tumors with little or no expression in benign ovarian tumors. We also noted that CDCP1 palmitoylation, which can occur at any one of four carboxyl terminal cysteines and is required for CDCP1 degradation but not internalization, is seen in mouse xenografts of an ovarian cancer cell line as well as patient tumors. Interestingly, we observed that CDCP1 levels were generally lower in the metastases than the matching primary tumor of 6 ovarian cancer patients. However, it is noteworthy that levels of palmitoylated CDCP1 were markedly lower in each of the metastases, compared with the matching primary tumor. These observations suggest that palmitoylation regulated cellular processing of CDCP1 is relevant *in vivo* including in the primary tumors and metastases of patients with high grade serous ovarian cancer. It is possible that the reduced palmitoylation of CDCP1 observed by us at metastatic sites is because of the localized impact of EGF. We speculate that in this setting EGF inhibits constitutive internalization and palmitoylation-dependent degradation of CDCP1 promoting its availability on the cell surface. Accordingly, our expectation is that CDCP1 will be predominantly located on the surface of metastatic ovarian cancer cells, as was seen by Razorenova et al for a sub-set of ccRCC patients (10).

We have shown previously that EGF induces relocalization of CDCP1 from cell-cell junctions to filopodia and intracellular stores and that blockade of CDCP1 via silencing or function blocking antibodies is effective at reducing EGF/EGFR-induced cell migration (23). Our current data provide insights into the kinetics of these events (Figure 6). Over short

periods (up to 1 h), CDCP1 internalizes at the same rate in both resting and EGF-stimulated cells (Figure 3D). Under basal conditions ~85% of internalized CDCP1 remains inside the cell (Figure 3D), and by 8 h most of this is degraded (Figure 3C) with near complete degradation by 12 h (Figure 1A). In contrast, EGF induces recycling of ~45% of internalized CDCP1 to the cell surface (Figure 3D) where it is protected (Fig 1A). Interestingly, palmitoylation of CDCP1 is essential for its degradation but not its internalization. In Figure 6 we have shown CDCP1 as palmitoylated at each cellular location as we do not yet know where its palmitoylation actually occurs. In addition to CDCP1 recycling to the cell surface, EGF causes movement of CDCP1 out of lipid raft containing membrane fractions (Figure 4C). Reduced lipid raft localization was accompanied by reduced tyrosine phosphorylation of CDCP1 (Figure 4D). This is consistent with EGF-induced movement of CDCP1 away from the membrane micro-domains known to harbor the key mediator of CDCP1 phosphorylation, Src. However, we noted that residual levels of pY-CDCP1 were 30-55% in the two cell lines we examined even after 24 h of EGF treatment. This suggests a level of compartmentalization of CDCP1 that permits its continued association with Src. Whether this level of Src associated CDCP1 is sufficient to continue oncogenic signalling needs to be examined. On the basis of the increased rate of migration induced by EGF in cells expressing palmitoylation-deficient CDCP1, it would appear that non-Src associated CDCP1 nevertheless may also possess oncogenic activity. However, the actual impact on CDCP1/Src-mediated signalling, and cancer progression overall, of EGF-induced transit of CDCP1 away from lipid rafts remains to be determined. In Figure 6 we represented CDCP1 recycling and lipid raft relocalization as separate events, although it is possible that these occur simultaneously. Interestingly, under basal conditions and in response to EGF, cells expressing palmitoylation-deficient CDCP1-4C migrated to a greater extent than cells expressing palmitoylation-competent CDCP1 (Figure 5). This likely reflects differences in the kinetics of trafficking of CDCP1 and CDCP1-4C. Our data indicate that both CDCP1 and CDCP1-4C are constitutively internalized with the kinetics of this process the same in the first hour (Figure 3D). In contrast, the rate of recycling to the cell surface is different. Whereas recycling of internalized CDCP1 is a regulated process requiring EGF signaling, for palmitoylation-deficient CDCP1 relocalization to the cell surface occurs constitutively, suggesting that representation of CDCP1-4C occurs more rapidly than CDCP1. The resulting more rapid kinetics of recycling of CDCP1-4C to the cell surface may explain why cells expressing palmitoylation-deficient CDCP1 migrate more rapidly than cells expressing the wildtype protein.

In summary, our data reveal the first example of the EGFR system functioning to increase the lifespan of a protein and to promote protein recycling to the cell surface. As the target of these effects, CDCP1, is readily disrupted with monoclonal antibodies that induce cancer cell death *in vivo* (18-20, 22), our data could be useful for the development of paradigms for treatment of EGFR-dependent cancer, potentially including dual targeting of EGFR and CDCP1.

MATERIAL AND METHODS

Antibodies, reagents and expression constructs

Antibodies were to CDCP1 (#4115), STAT3, phospho-STAT3 (Y705), NFκB, phospho-NFκB (S536) (Cell Signaling Technology), caveolin-1, a pY20 antibody directed against tyrosine phosphorylated proteins (Santa Cruz Biotechnology), Flottilin-1 (BD Biosciences) and GAPDH (Sigma Aldrich). IRDye680- and 800-conjugated secondary antibodies (LiCor), Alexa Fluor-488 conjugated secondary antibody, Alexa Fluor-568 conjugated phalloidin, 4'-6-diamidino-2-phenylindole (DAPI) and cell culture media and reagents were from Invitrogen, fetal calf serum (FCS) from Sigma Aldrich, protease inhibitor cocktail from Roche, and EZ-link NHS-SS-biotin and EZ-link HPDP-biotin from Pierce. The CDCP1-FLAG-pcDNA3.1 mammalian expression construct has been described (4). Mutation of C689, C690, C772 and C780 to alanine used Pfu Ultra polymerase (Agilent Technologies). The sequence of constructs was confirmed by DNA sequencing (AGRF).

Cell culture, transfections and treatments and collection of lysates

Cells were from ATCC, except SKOV3 cells which were from Cell Biolabs. Cells were non-enzymatically dissociated using 0.5 mM EDTA in PBS. Transfections used Lipofectamine 2000 (Invitrogen). For treatments, cells at 70% confluence grown in serum free media for 24 h were incubated in media containing 0.1% DMSO (vehicle control) or 0.1% DMSO with EGF (30 ng/ml), IL-6 (50 ng/ml) or TNFα (50 ng/ml). MG132 (20 μM) in culture media inhibited protein degradation. Cells washed with PBS were lysed in 50 mM HEPES pH 7.4, 150 mM NaCl, 5 mM EDTA, 1% Triton X-100 (v/v), 1 x protease inhibitor cocktail (Roche)).

Mouse xenograft tumors

Animal experiments were approved by the University of Queensland Animal Ethics Committee. Tumours were harvested 5 weeks after female NOD SCID gamma mice (Jackson Laboratories) were injected subcutaneously or intraperitoneally with ovarian cancer SKOV3 cells (2 x 10^6).

Patient tissue

Research involving human subjects was approved by the Mater Health Services Human Research Ethics Committee. Informed consent was obtained from all subjects. Tissue was collected prospectively from June 2012 to July 2013 from women with benign gynaecological disorders undergoing oophorectomy and women treated surgically for high grade serous ovarian cancer. Lysates were collected from tissue snap frozen in liquid nitrogen then pulverized before addition of lysis buffer.

Analysis of palmitoylation by acyl-biotinyl exchange chemistry

CDCP1 palmitoylation was examined using a previously described acyl-biotinyl exchange assay (27). To ensure that all 10 of the CDCP1 disulfide bonds were reduced and available for labelling, DTT (1 mM) was included in the step in which N-ethylmaleimide (NEM; 10 mM) was reacted with free thiol groups. As a control, tris pH 8.0 was substituted for hydroxylamine, the reagent which chemically cleaves endogenous palmitate from proteins. Assays were performed at least 3 times and examined by Western blot analysis. Densitometric signals from Western blot analysis at each EGF treatment time point were normalized to the signal from untreated cells and the average ratio (+/- SD) of palmitoylated to total CDCP1 displayed graphically to monitor the relative change in palmitoylated CDCP1 in response to EGF.

Degradation, internalisation and recycling assays

Cell surface proteins were labelled with cell impermeant EZ-link-NHS-SS-biotin (0.5 mg/ml) for 30 min at 4°C (27). For all assays, biotinylated proteins were affinity isolated from whole cell lysates at defined time points using streptavidin beads. To assess CDCP1 lifetime, after biotinylation cells were incubated at 37°C for 0.5, 1, 2 and 8 h, before collection of lysates. To examine the role of protein degradation in loss of biotinylated CDCP1, cells were incubated in media containing the proteasome inhibitor MG132 (20 μM) for the final 6 h of an 8 h time point. To examine CDCP1 internalization, after biotinylation, cells were

incubated at 37°C in culture media for 1 h before residual biotin was removed from cell surface proteins using the reducing agent MeSNA (50 mM) in a Tris (pH 8.6, 100 mM), NaCl (100 mM) buffer for 30 min. A quenching buffer of 60 mM iodoacetamide in PBS was added for 15 min before whole cell lysates were collected. To examine CDCP1 recycling to the cell surface, the same protocol used to examine internalization was followed, except that after removal of residual cell surface biotin with MeSNA and subsequent quenching, cells were incubated at 37°C for a further 1 h before biotinylated proteins that had recycled to the cell surface were removed by a second round of treatment with MeSNA followed by quenching before collection of whole cell lysates. Biotinylated proteins were affinity purified as described above and equivalent volumes examined by Western blot analysis. Assays were performed at least 3 times. The average densitometric signal (+/- SD) from Western blot analysis of each assay at each time point was used to calculate: (i) percentage of intracellular CDCP1 = (CDCP1 at relevant time point – CDCP1 at t=0)/(CDCP1 immediately after cell surface biotinylation (S)) x 100; and (ii) percentage of CDCP1 recycled to cell surface = 100 – [((CDCP1 level after first round of 37°C) – (CDCP1 level after second round of 37°C))/((CDCP1 level after first round of 37°C) – (CDCP1 level at 0 time)) × 100] (30).

Detergent-free membrane fraction isolation by density separation and ultracentrifugation

Membrane fractions were isolated as previously described from cells lysed in 20 mM Tris, pH 7.5, 250 mM sucrose, 1 mM $CaCl_2$, 1 mM $MgCl_2$ and 1 x protease inhibitor cocktail (35, 36). Assays were performed 3 times and the average densitometric signal (+/- SD) from Western blot analysis of each fraction was used to calculate the percentage of CDCP1 in each using the formula: [(CDCP1 in relevant fraction)/(combined CDCP1 from all fractions)] x 100.

Immunoprecipitation

Immunoprecipitations were performed as previously described (4) using a rabbit anti-CDCP1 antibody (#4115 (1:100)). Immunoprecipitated proteins were probed by Western blot analysis using the mouse monoclonal pY20 antibody. Experiments were performed 3 times with densitometric analysis performed to calculate phosphorylated CDCP1 relative to total CDCP1.

Western blot analysis

Equal amounts of whole cell lysates, tissue lysates, proteins eluted from streptavidin beads, proteins collected from cell surface biotinylation protocols, immunoprecipitated proteins and membrane fractions were examined by Western blot analysis as previously described (4). Signal was detected by scanning membranes using an Odyssey infrared imaging system (LiCor). Membranes were reprobed with an anti-GAPDH or anti-actin antibody. Where needed, signal intensity was quantified by densitometry using Odyssey software (LiCor). Western blot images are representative of experiments performed at least 3 times.

Confocal microscopy

Confocal microscopy was performed on permeabilized cells as previously described (37) using the M2 mouse anti-FLAG antibody (1:600 dilution) and a Zeiss LSM510 confocal microscope. Images were processed using Corel Draw X5.

Cell migration

Cells (5×10^5) seeded in serum free media into the top well of modified Transwell chambers containing a polycarbonate nucleopore membrane (Corning) migrated over 48 hours towards a 1% FCS gradient. For stimulation, EGF (30 ng/ml) was added to the top well at the time of seeding. Migrated cells attached at the bottom of the well were fixed with methanol, stained with 0.2% crystal violet and 4 fields counted at x100 per well. Assays were performed 3 times in triplicate and the average number of migrated cells (+/- SD) graphed.

Statistical analysis

All assays were performed on at 3 times and results are mean ± SD. Statistical significance was assessed by Student's t test in all experiments, with the exception of migration assays where significance was assessed using a one-way ANOVA test. $P < 0.05$ was considered significant.

CONFLICT OF INTEREST

JDH is an inventor on a patent describing CDCP1 as an anti-cancer target. All other authors declare no conflicts of interest.

ACKNOWLEDGEMENTS

We thank Dr Jon Whitehead for helpful discussions. This work was supported by Cancer Council Queensland grants 614205 and 1021827 and Wesley Research Institute grant 2008/06 to JDH. MNA and BSH received Australian Post-Graduate Awards. JDH holds Australian Research Council Future Fellowship FT120100917.

REFERENCES

1. Ciardiello F, Tortora G. EGFR antagonists in cancer treatment. N Engl J Med. 2008; 358(11):1160-74.
2. Holohan C, Van Schaeybroeck S, Longley DB, Johnston PG. Cancer drug resistance: an evolving paradigm. Nat Rev Cancer. 2013; 13(10):714-26.
3. Wheeler DL, Dunn EF, Harari PM. Understanding resistance to EGFR inhibitors-impact on future treatment strategies. Nat Rev Clin Oncol. 2010; 7(9):493-507.
4. He Y, Wortmann A, Burke LJ, Reid JC, Adams MN, Abdul-Jabbar I, et al. Proteolysis-induced N-terminal ectodomain shedding of the integral membrane glycoprotein CUB domain-containing protein 1 (CDCP1) is accompanied by tyrosine phosphorylation of its C-terminal domain and recruitment of Src and PKCδ. J Biol Chem. 2010; 285(34):26162-73.
5. Uekita T, Sakai R. Roles of CUB domain-containing protein 1 signaling in cancer invasion and metastasis. Cancer Sci. 2011; 102(11):1943-8.
6. Wortmann A, He Y, Deryugina EI, Quigley JP, Hooper JD. The cell surface glycoprotein CDCP1 in cancer--insights, opportunities, and challenges. IUBMB Life. 2009; 61(7):723-30.
7. Hooper JD, Zijlstra A, Aimes RT, Liang H, Claassen GF, Tarin D, et al. Subtractive immunization using highly metastatic human tumor cells identifies SIMA135/CDCP1, a 135 kDa cell surface phosphorylated glycoprotein antigen. Oncogene. 2003; 22(12):1783-94.
8. Awakura Y, Nakamura E, Takahashi T, Kotani H, Mikami Y, Kadowaki T, et al. Microarray-based identification of CUB-domain containing protein 1 as a potential prognostic marker in conventional renal cell carcinoma. J Cancer Res Clin Oncol. 2008; 134(12):1363-9.
9. Emerling BM, Benes CH, Poulogiannis G, Bell EL, Courtney K, Liu H, et al. Identification of CDCP1 as a hypoxia-inducible factor 2alpha (HIF-2alpha) target gene that is associated with survival in clear cell renal cell carcinoma patients. Proc Natl Acad Sci U S A. 2013; 110(9):3483-8.

10. Razorenova OV, Finger EC, Colavitti R, Chernikova SB, Boiko AD, Chan CK, et al. VHL loss in renal cell carcinoma leads to up-regulation of CUB domain-containing protein 1 to stimulate PKCδ-driven migration. Proc Natl Acad Sci U S A. 2011; 108(5):1931-6.
11. Miyazawa Y, Uekita T, Hiraoka N, Fujii S, Kosuge T, Kanai Y, et al. CUB domain-containing protein 1, a prognostic factor for human pancreatic cancers, promotes cell migration and extracellular matrix degradation. Cancer Res. 2010; 70(12):5136-46.
12. Ikeda J, Oda T, Inoue M, Uekita T, Sakai R, Okumura M, et al. Expression of CUB domain containing protein (CDCP1) is correlated with prognosis and survival of patients with adenocarcinoma of lung. Cancer Sci. 2009; 100(3):429-33.
13. Gao W, Chen L, Ma Z, Du Z, Zhao Z, Hu Z, et al. Isolation and phenotypic characterization of colorectal cancer stem cells with organ-specific metastatic potential. Gastroenterology. 2013; 145(3):636-46 e5.
14. Uekita T, Jia L, Narisawa-Saito M, Yokota J, Kiyono T, Sakai R. CUB domain-containing protein 1 is a novel regulator of anoikis resistance in lung adenocarcinoma. Mol Cell Biol. 2007; 27(21):7649-60.
15. Liu H, Ong SE, Badu-Nkansah K, Schindler J, White FM, Hynes RO. CUB-domain-containing protein 1 (CDCP1) activates Src to promote melanoma metastasis. Proc Natl Acad Sci U S A. 2011; 108(4):1379-84.
16. Uekita T, Tanaka M, Takigahira M, Miyazawa Y, Nakanishi Y, Kanai Y, et al. CUB-domain-containing protein 1 regulates peritoneal dissemination of gastric scirrhous carcinoma. Am J Pathol. 2008; 172(6):1729-39.
17. Deryugina EI, Conn EM, Wortmann A, Partridge JJ, Kupriyanova TA, Ardi VC, et al. Functional role of cell surface CUB domain-containing protein 1 in tumor cell dissemination. Mol Cancer Res. 2009; 7(8):1197-211.
18. Casar B, He Y, Iconomou M, Hooper JD, Quigley JP, Deryugina EI. Blocking of CDCP1 cleavage in vivo prevents Akt-dependent survival and inhibits metastatic colonization through PARP1-mediated apoptosis of cancer cells. Oncogene. 2012; 31(35):3924-38.
19. Casar B, Rimann I, Kato H, Shattil SJ, Quigley JP, Deryugina EI. In vivo cleaved CDCP1 promotes early tumor dissemination via complexing with activated beta1 integrin and induction of FAK/PI3K/Akt motility signaling. Oncogene. 2013 Dec 3.
20. Fukuchi K, Steiniger SC, Deryugina E, Liu Y, Lowery CA, Gloeckner C, et al. Inhibition of tumor metastasis: functional immune modulation of the CUB domain containing protein 1. Mol Pharm. 2010; 7(1):245-53.

21. Kollmorgen G, Niederfellner G, Lifke A, Spohn GJ, Rieder N, Vega Harring S, et al. Antibody mediated CDCP1 degradation as mode of action for cancer targeted therapy. Mol Oncol. 2013 Sep 3.
22. Siva AC, Wild MA, Kirkland RE, Nolan MJ, Lin B, Maruyama T, et al. Targeting CUB domain-containing protein 1 with a monoclonal antibody inhibits metastasis in a prostate cancer model. Cancer Res. 2008; 68(10):3759-66.
23. Dong Y, He Y, de Boer L, Stack MS, Lumley JW, Clements JA, et al. The cell surface glycoprotein CUB domain-containing protein 1 (CDCP1) contributes to epidermal growth factor receptor-mediated cell migration. J Biol Chem. 2012; 287(13):9792-803.
24. Yarden Y, Sliwkowski MX. Untangling the ErbB signalling network. Nat Rev Mol Cell Biol. 2001; 2(2):127-37.
25. Kulbe H, Chakravarty P, Leinster DA, Charles KA, Kwong J, Thompson RG, et al. A dynamic inflammatory cytokine network in the human ovarian cancer microenvironment. Cancer Res. 2012; 72(1):66-75.
26. Blaskovic S, Blanc M, van der Goot FG. What does S-palmitoylation do to membrane proteins? FEBS J. 2013; 280(12):2766-74.
27. Adams MN, Christensen ME, He Y, Waterhouse NJ, Hooper JD. The role of palmitoylation in signalling, cellular trafficking and plasma membrane localization of protease-activated receptor-2. PLoS One. 2011; 6(11):e28018.
28. Adams MN, Pagel CN, Mackie EJ, Hooper JD. Evaluation of antibodies directed against human protease-activated receptor-2. Naunyn Schmiedebergs Arch Pharmacol. 2012; 385(9):861-73.
29. Dietzen DJ, Hastings WR, Lublin DM. Caveolin is palmitoylated on multiple cysteine residues. Palmitoylation is not necessary for localization of caveolin to caveolae. J Biol Chem. 1995; 270(12):6838-42.
30. Joffre C, Barrow R, Menard L, Calleja V, Hart IR, Kermorgant S. A direct role for Met endocytosis in tumorigenesis. Nat Cell Biol. 2011; 13(7):827-37.
31. Miyazawa Y, Uekita T, Ito Y, Seiki M, Yamaguchi H, Sakai R. CDCP1 regulates the function of MT1-MMP and invadopodia-mediated invasion of cancer cells. Mol Cancer Res. 2013; 11(6):628-37.
32. Benes CH, Wu N, Elia AE, Dharia T, Cantley LC, Soltoff SP. The C2 domain of PKCδ is a phosphotyrosine binding domain. Cell. 2005; 121(2):271-80.
33. Sandilands E, Frame MC. Endosomal trafficking of Src tyrosine kinase. Trends Cell Biol. 2008; 18(7):322-9.

34. Rosell R, Carcereny E, Gervais R, Vergnenegre A, Massuti B, Felip E, et al. Erlotinib versus standard chemotherapy as first-line treatment for European patients with advanced EGFR mutation-positive non-small-cell lung cancer (EURTAC): a multicentre, open-label, randomised phase 3 trial. Lancet Oncol. 2012; 13(3):239-46.
35. Macdonald JL, Pike LJ. A simplified method for the preparation of detergent-free lipid rafts. J Lipid Res. 2005; 46(5):1061-7.
36. Morris DP, Lei B, Wu YX, Michelotti GA, Schwinn DA. The alpha1a-adrenergic receptor occupies membrane rafts with its G protein effectors but internalizes via clathrin-coated pits. J Biol Chem. 2008; 283(5):2973-85.
37. Wortmann A, He Y, Christensen ME, Linn M, Lumley JW, Pollock PM, et al. Cellular settings mediating Src Substrate switching between focal adhesion kinase tyrosine 861 and CUB-domain-containing protein 1 (CDCP1) tyrosine 734. J Biol Chem. 2011; 286(49):42303-15.

FIGURE LEGENDS

Figure 1. EGF protects CDCP1 from degradation. (**a**) *Upper*, Western blot for CDCP1 of biotinylated proteins and lysates from Caov3 and OVCA420 cells immediately after cell surface biotinylation (S) or after 12 h +/- EGF (30 ng/ml). Densitometric analysis of total CDCP1 relative to untreated (S) is displayed numerically below 'Total CDCP1' blot. *Lower*, Graph of the percentage of biotinylated CDCP1 in CaOV3 (black bar) and OVCA420 (grey bar) cells remaining after 12 h +/- EGF. * $P<0.05$. (**b**) Western blot for CDCP1 of biotinylated proteins and lysates from OVCA420 cells immediately after cell surface biotinylation (S) or after 12 h +/- either IL-6 (50 ng/ml) or TNFα- (50 ng/ml). Anti-STAT3, -p-STAT3-Y705, -NFκB and -p-NFκB-S536 Western blots indicate that IL-6 and TNFα induced signaling. Arrow and arrowhead, 135 kDa and 70 kDa CDCP1, respectively. Only 135 kDa CDCP1 from lysates is shown.

Figure 2. CDCP1 is palmitoylated. (**a**) Sequence of transmembrane (underline) and carboxyl terminal domains of CDCP1 showing cysteines (red) and tyrosine 734, 743 and 762 (blue). (**b**) Anti-CDCP1 and CAV1 Western blot of palmitoylated proteins and total lysates from prostate DU145, PC-3 and 22Rv1, ovarian Caov3 and OVCA420, gastric MKN7, kidney 786-O and lung A549 cancer cells. (**c**) *Upper*, Mouse subcutaneous SKOV3 cell tumor (dotted circle) and intraperitoneal SKOV3 cell tumors (dotted circle). *Lower*, Western blot for

CDCP1 of palmitoylated and total CDCP1 from lysates of SKOV3 cell grown *in vitro* or as subcutaneous or intraperitoneal tumors in mice. (**d**) Western blot for CDCP1 of palmitoylated proteins and lysates from tissues from 7 women with benign ovarian tumors and 9 women with high grade serous ovarian cancer. Patient details are provided in Table S1. *, non-specific signal due to cross-reactivity of the secondary antibody. (**e**) Western blot for CDCP1 of palmitoylated proteins and lysates from matching primary tumours and omental metastases from 4 women with high grade serous ovarian cancer. (**f**) Western blot for CDCP1 of palmitoylated proteins and lysates from HeLa cells transiently expressing wildtype or mutated CDCP1 where C1A is C689A, C2A is C690A, C3A is C772A, and C4A is C780A. Arrow and arrowhead, 135 kDa and 70 kDa CDCP1, respectively.

Figure 3. EGF inhibits palmitoylation-dependent proteasomal degradation of CDCP1 promoting its recycling to the cell surface. HeLa cells transiently expressed CDCP1 (WT) or CDCP1-4C (4C). (**a**) *Left*, Confocal microscopy. Green, CDCP1. Red, actin. Blue, nuclei. *Centre*, Western blot for CDCP1 of biotinylated proteins and lysates immediately after cell surface biotinylation (S) or after incubation at 37°C for 6, 12 and 24 h. *Right*, Graph of CDCP1 levels at each time point (* $P<0.01$). (**b**) *Left*, Western blot for CDCP1 of biotinylated proteins and lysates immediately after cell surface biotinylation (S) or 12 h later +/- EGF (30 ng/ml). *Right*, Graph of the percentage of biotinylated CDCP1 (black bar) and CDCP1-4C (grey bar) remaining after 12 h +/- EGF (* $P<0.05$). (**c**) *Upper*, Scheme of the experimental protocol. *Middle*, Western blot for CDCP1 of cell surface biotinylated proteins internalized after 0.5, 1, 2 and 8 h. To examine whether reduced levels of CDCP1 are due to proteasomal degradation, cells were co-incubated for the final 6 h of an 8 h timepoint with proteasome inhibitor MG132 for 8 h. Densitometric analysis was performed for the 8 h time points from 3 independent experiments and is displayed below the blot. *Lower*, Graph of internalized CDCP1 remaining at each time point (** $P<0.01$). (**d**) *Upper*, Scheme of the experimental protocol. *Middle*, Western blot for CDCP1 of internalized cell surface biotinylated proteins after 1 h (Int.) and proteins that did not recycle to the cell surface after a further 1h (Unrec.). *Lower*, Graph of the percentage of CDCP1 (black bar) and CDCP1-4C (grey bar) that recycled to the cell surface after the second 1 h incubation. Arrow, 135 kDa CDCP1. Proteolytic processing of CDCP1 transiently expressed by HeLa cells is generally not apparent from Western blot analysis. * $P<0.05$.

Figure 4. EGF reduces CDCP1 palmitoylation and promotes its redistribution into non-lipid raft membrane fractions. (**a**) *Upper*, Western blot for CDCP1 of palmitoylated proteins and total lysates from OVCA420 and Caov3 cells +/- EGF (30 ng/ml). *Lower*, Graph of palmitoylated to total CDCP1. (* $P<0.01$) (**b**) Western blot for CDCP1 of palmitoylated proteins and total lysates from HeLa cells transiently expressing wildtype CDCP1 +/- EGF (30 ng/ml). Cells had been transfected overnight before EGF treatments commenced. (**c**) *Upper*, Anti-CDCP1 and Flottilin-1 Western blot of membrane fractions 1-5 from untreated (- EGF) and EGF treated (30 ng/ml; + EGF) Caov3 cells. *Lower*, Graph of densitometry analysis of 3 independent experiments showing the percentage of CDCP1 present in each fraction. (** $P<0.05$). (**d**) Western blot for tyrosine phosphorylated and total CDCP1 immunoprecipitated from lysates of OVCA420 and Caov3 cells +/- EGF (30 ng/ml). Densitometric analysis of tyrosine phosphorylated CDCP1 relative to total CDCP1 is displayed numerically below the total CDCP1 blot. Arrow and arrowhead, 135 kDa and 70 kDa CDCP1, respectively.

Figure 5. Palmitoylation retards basal and EGF-induced CDCP1-mediated cell migration. Cells seeded into the top well of a Transwell chamber migrated over 48 hours towards 1% FCS +/-EGF (30 ng/ml). * $P<0.05$.

Figure 6. Schematic representation of mechanisms involved in CDCP1 internalization, degradation and recycling. In unstimulated cells CDCP1, expressed at basal levels, is constitutively internalized and degraded. Internalization is palmitoylation-independent while CDCP1 degradation requires its palmitoylation. As the cellular location where CDCP1 palmitoylation occurs is not yet known, each representation of the protein is palmitoylated (green line). Under basal conditions, palmitoylation is represented as a thick green line embedded in the lipid bilayer. EGF via the EGFR system stimulates expression of CDCP1, inhibits its degradation and also promotes its recycling to the cell surface. As recycling to the cell surface predominates over degradation, palmitoylation is represented with a thin green line under conditions where EGF is present. Under basal conditions, CDCP1 is predominantly located in lipid rafts (green lipid bilayer), whereas EGF induces CDCP1 translocation into lipid-poor membrane fractions (orange lipid bilayer).

Figure 1

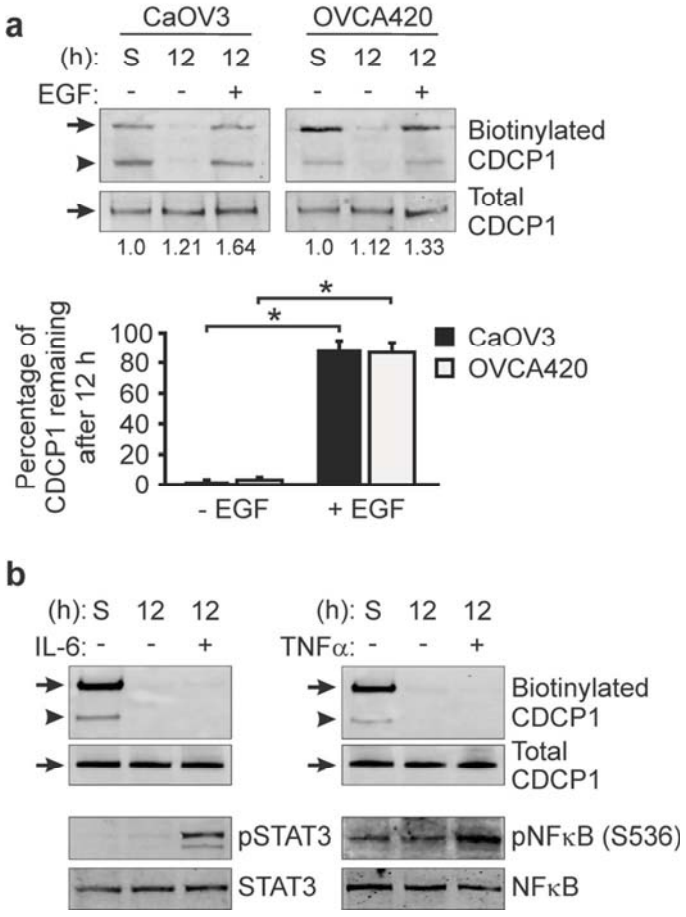
a
CaOV3
OVCA420
(h): S 12 12 S 12 12
EGF: - - + - - +
Biotinylated CDCP1
Total CDCP1
1.0 1.21 1.64 1.0 1.12 1.33
Percentage of CDCP1 remaining after 12 h
100
80
60
40
20
0
*
*
CaOV3
OVCA420
- EGF
+ EGF
b
(h): S 12 12
IL-6: - - +
(h): S 12 12
TNFα: - - +
Biotinylated CDCP1
Total CDCP1
pSTAT3
STAT3
pNFκB (S536)
NFκB

Figure 2

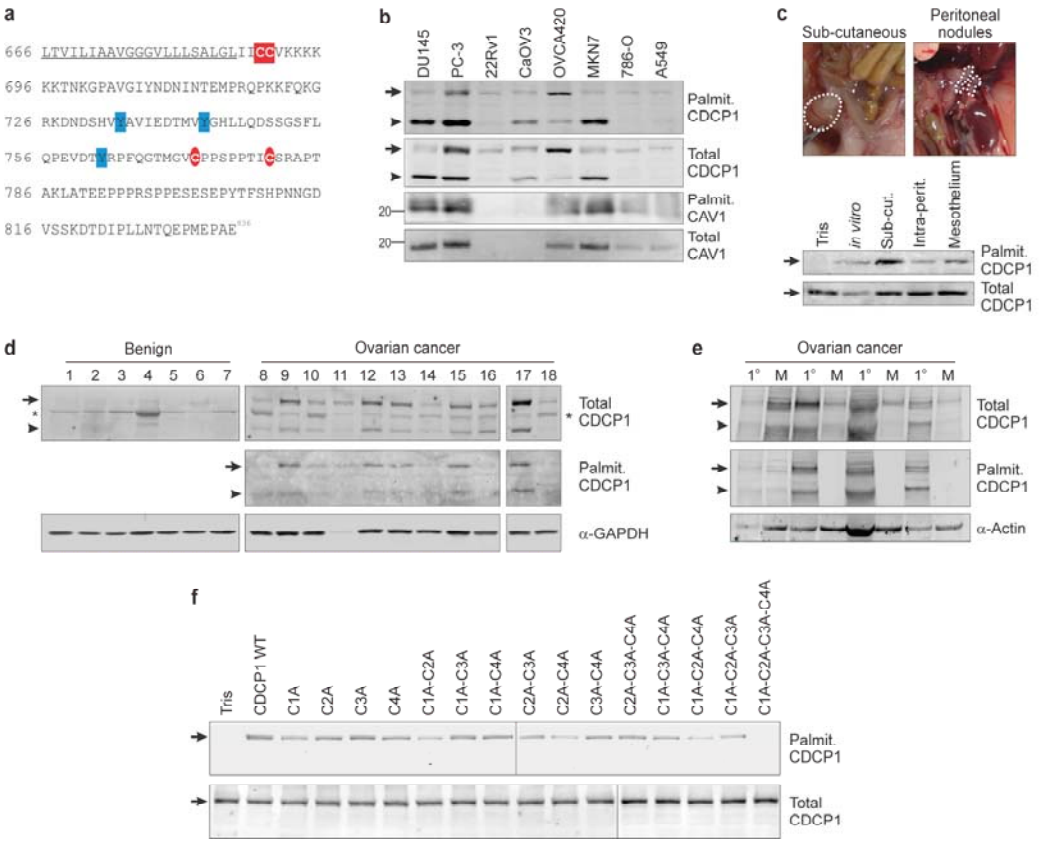
a
666 LTVILIAAVGGGVLLLSALGLIICCVKKK
696 KKTNKGPAVGIYNDNINTEMPRQPKKFQKG
726 RKDNDSHVSAVIEDTMVDGHLLQDSSGSFL
756 QPEVDTKRPFQGTMGVCPPSPPTICSRAPT
786 AKLATEEPPPRSPPESESEPYTFSHPNNGD
816 VSSKDTDIPLLNTQEPMEPAE836
b
DU145
PC-3
22Rv1
CaOV3
OVCA420
MKN7
786-O
A549
Palmit. CDCP1
Total CDCP1
Palmit. CAV1
Total CAV1
20
20
c
Sub-cutaneous
Peritoneal nodules
Tris
in vitro
Sub-cu.
Intra-perit.
Mesothelium
Palmit. CDCP1
Total CDCP1
d
Benign
Ovarian cancer
1 2 3 4 5 6 7 8 9 10 11 12 13 14 15 16 17 18
Total CDCP1
Palmit. CDCP1
α-GAPDH
e
Ovarian cancer
1° M 1° M 1° M 1° M
Total CDCP1
Palmit. CDCP1
α-Actin
f
Tris
CDCP1 WT
C1A
C2A
C3A
C4A
C1A-C2A
C1A-C3A
C1A-C4A
C2A-C3A
C2A-C4A
C3A-C4A
C2A-C3A-C4A
C1A-C3A-C4A
C1A-C2A-C4A
C1A-C2A-C3A
C1A-C2A-C3A-C4A
Palmit. CDCP1
Total CDCP1

Figure 3

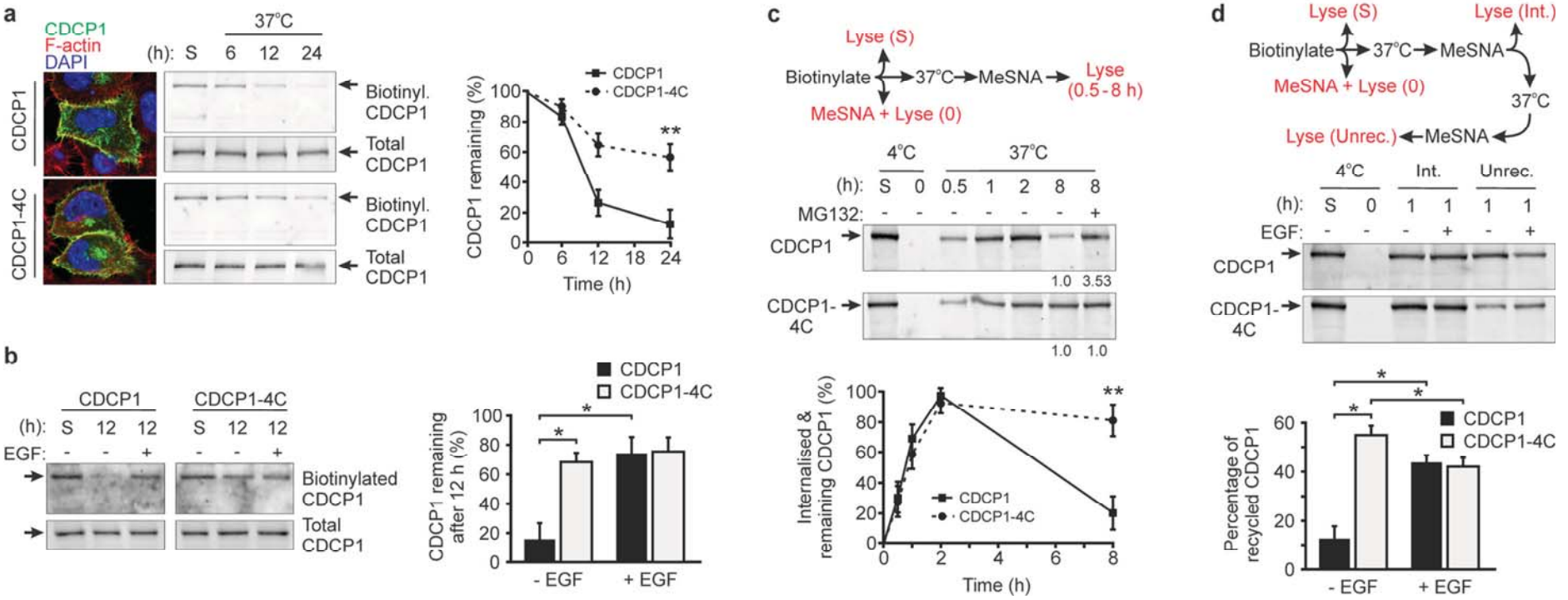
a
CDCP1
F-actin
DAPI
37°C
(h): S 6 12 24
CDCP1
CDCP1-4C
Biotinyl. CDCP1
Total CDCP1
Biotinyl. CDCP1
Total CDCP1
CDCP1 remaining (%)
CDCP1
CDCP1-4C
**
Time (h)
b
CDCP1
CDCP1-4C
(h): S 12 12 S 12 12
EGF: - - + - - +
Biotinylated CDCP1
Total CDCP1
CDCP1 remaining after 12 h (%)
CDCP1
CDCP1-4C
- EGF
+ EGF
c
Lyse (S)
Biotinylate
37°C
MeSNA
Lyse (0.5 - 8 h)
MeSNA + Lyse (0)
4°C
37°C
(h): S 0 0.5 1 2 8 8
MG132: - - - - - - +
CDCP1
1.0 3.53
CDCP1-4C
1.0 1.0
Internalised & remaining CDCP1 (%)
CDCP1
CDCP1-4C
**
Time (h)
d
Lyse (S)
Lyse (Int.)
Biotinylate
37°C
MeSNA
MeSNA + Lyse (0)
37°C
Lyse (Unrec.)
MeSNA
4°C
Int.
Unrec.
(h): S 0 1 1 1 1
EGF: - - - + - +
CDCP1
CDCP1-4C
Percentage of recycled CDCP1
CDCP1
CDCP1-4C
- EGF
+ EGF

Figure 4

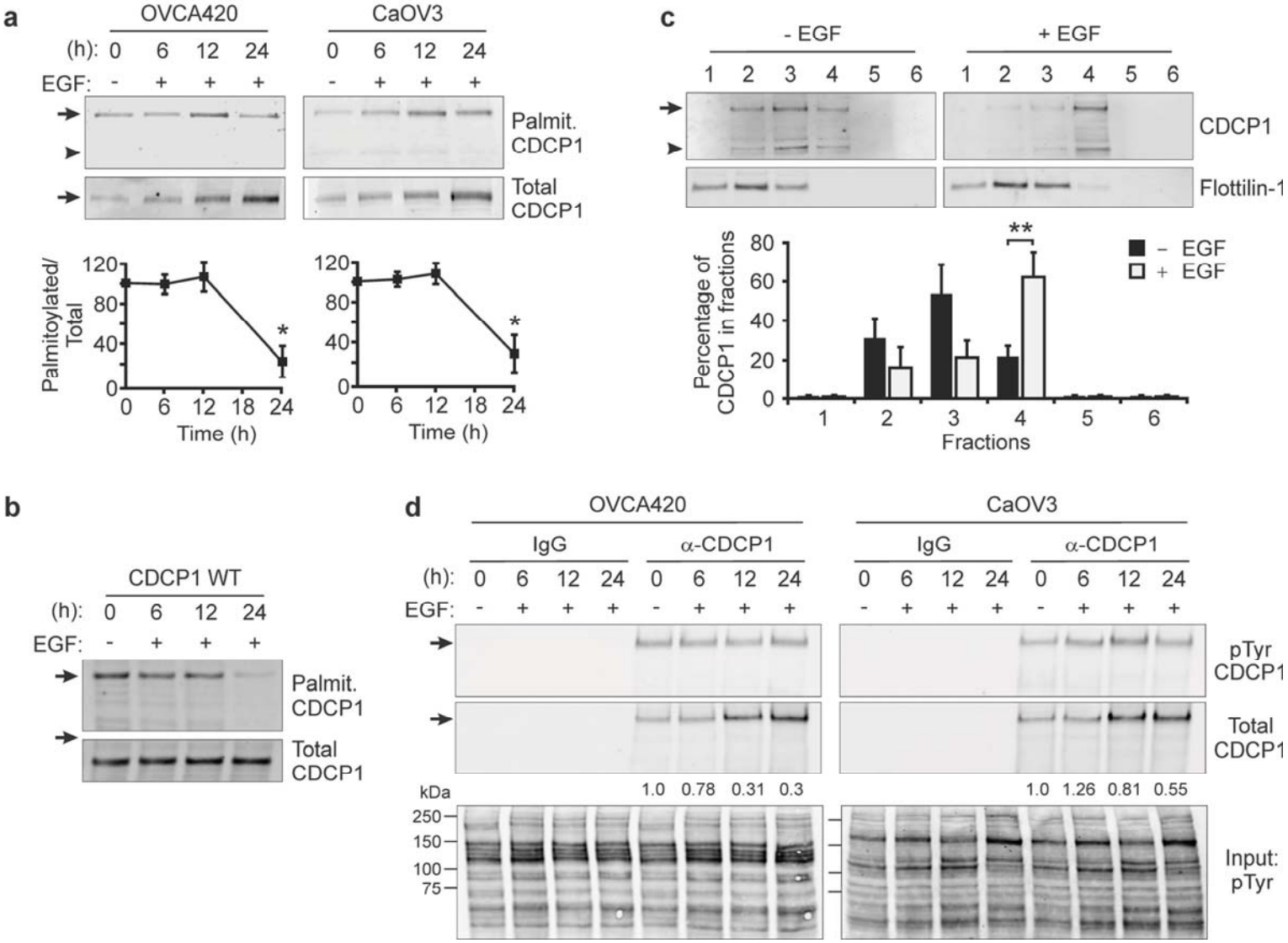
a
OVCA420
CaOV3
(h): 0 6 12 24 0 6 12 24
EGF: - + + + - + + +
Palmit. CDCP1
Total CDCP1
Palmitoylated/ Total
Time (h)
b
CDCP1 WT
(h): 0 6 12 24
EGF: - + + +
Palmit. CDCP1
Total CDCP1
c
- EGF
+ EGF
1 2 3 4 5 6
CDCP1
Flottilin-1
Percentage of CDCP1 in fractions
– EGF
+ EGF
Fractions
d
OVCA420
CaOV3
IgG
α-CDCP1
(h): 0 6 12 24 0 6 12 24
EGF: - + + + - + + +
pTyr CDCP1
Total CDCP1
1.0 0.78 0.31 0.3
1.0 1.26 0.81 0.55
kDa
250
150
100
75
Input: pTyr

Figure 5

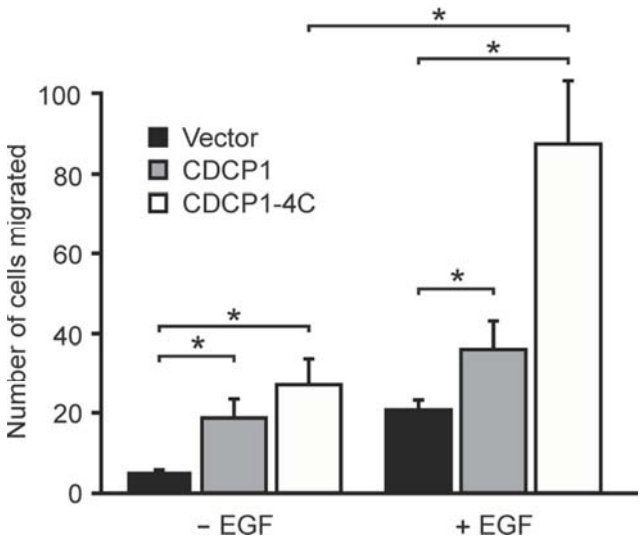
Number of cells migrated
100
80
60
40
20
0
Vector
CDCP1
CDCP1-4C
*
*
*
*
*
– EGF
+ EGF

Figure 6

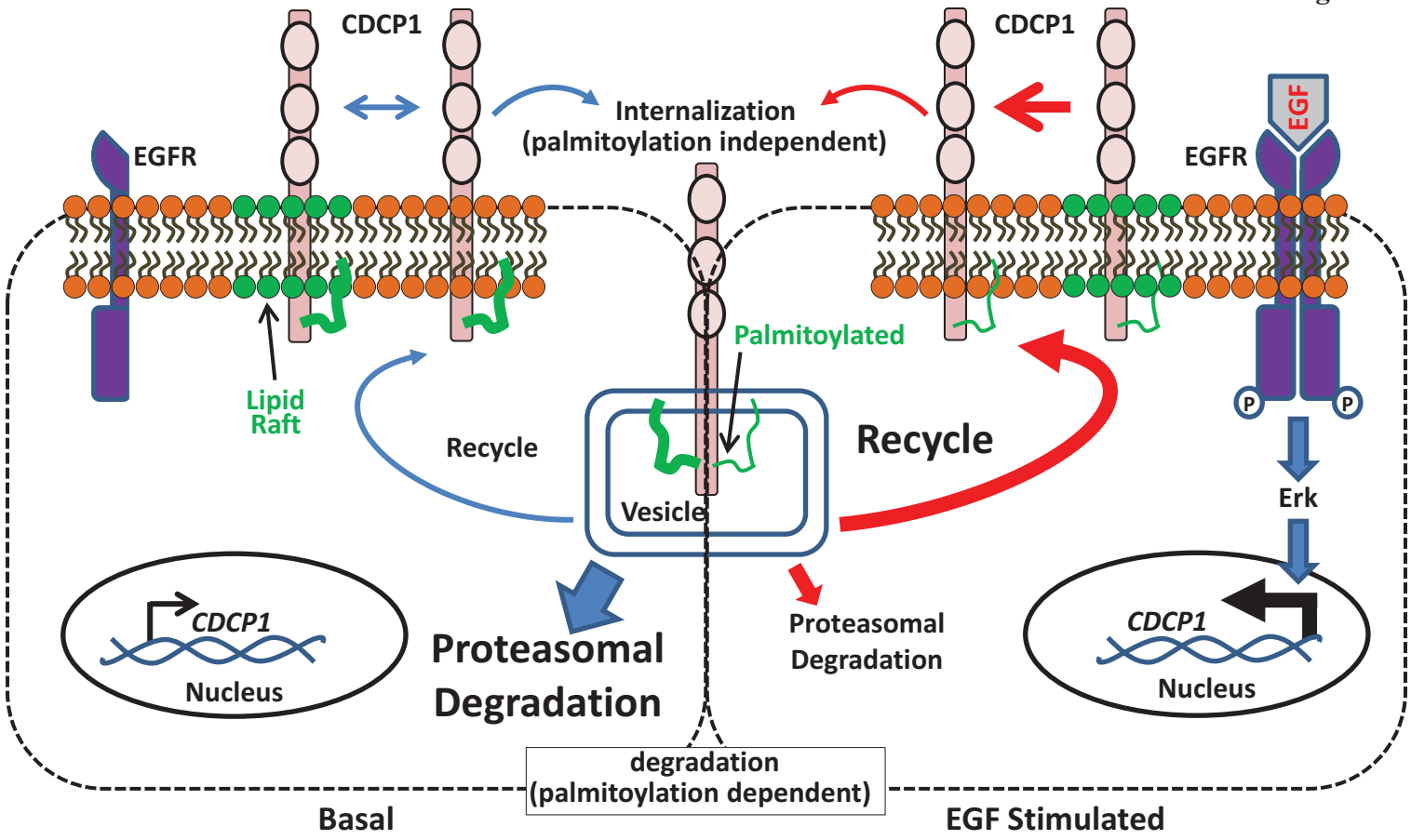
CDCP1
CDCP1
Internalization
(palmitoylation independent)
EGFR
EGFR
EGF
Palmitoylated
Lipid
Raft
Recycle
Recycle
Vesicle
P
P
Erk
CDCP1
Nucleus
Proteasomal
Degradation
Proteasomal
Degradation
CDCP1
Nucleus
degradation
(palmitoylation dependent)
Basal
EGF Stimulated

Table S1. Details of ovarian samples used in Fig. 2D.

			High grade serous ovarian cancer	
Lane	Benign ovary	Lane	Stage	Site[(1)]
1	serous cystadenofibroma	8	IIIC	Omentum
2	Endometriosis with cyst formation	9	IIIC	Ovary
3	Mucinous cystadenoma	10	IIIC	Pelvis
4	chronic endometritis	11	IIC	Ovary
5	Serous cystadenofibroma	12	IIC	Ovary
6	Benign mucinous cystadenoma	13	Unstaged	Omentum
7	Endometriosis	14	IIC	Omentum
		15	IIIC	Ovary[(2)]
		16	IIIC	Pelvis[(2)]
		17	IIIC	Ovary[(3)]
		18	IIIC	Omentum[(3)]

Footnotes:
(1) Site where specimen was taken from.
(2) Same patient
(3) Same patient. Sample used in lane 18 was collected after chemotherapy.